Skin-Core Structure–Fatigue Behavior Relationships for Injection-Molded Parts of Polypropylene. II. Morphology–Fatigue Behavior Relationships

JEAN-PIERRE TROTIGNON and JACQUES VERDU, *Ecole Nationale Supérieure d'Arts et Métiers, Département Materiaux, 151 Boulevard de l'Hôpital, 75640 PARIS Cedex 13, France*

Synopsis

The flexural fatigue properties were studied for PP injection-molded samples of different molecular weight and well-defined skin-core morphology (see Part I). It can be clearly seen that the crack initiation always occurs in the subskin layer of higher macromolecular orientation, and propagates towards the core. The mechanisms of cracking are discussed on the basis of fatigue kinetic data and analytical measurements on the stressed sections. The important influence of processing conditions, essentially holding pressure on the fatigue behavior is illustrated.

INTRODUCTION

It is well known that, in cyclic fatigue, two modes of failure can be involved. When the stress amplitude, the cycle frequency, and/or the sample thickness are too high, the dissipated energy cannot be efficiently evacuated, the temperature increases continuously, and a "thermal failure" occurs by pseudomelting. In less severe conditions, the material can reach a thermal equilibrium and the lifetime is governed by the crack initiation and propagation.

In the case of polypropylene (PP), most of the published work was devoted to the first mode and its transition to the second one,[1] the latter being essentially studied on notched specimens.[2] Thus a very small number of publications are available on the unnotched PP fatigue in "soft" conditions, although this probably corresponds to the most frequent used practical case.

The industrial parts of PP are generally made by injection molding, a process which leads to noticeable morphological heterogeneïties as shown in the first part of this paper. Then, a purely mechanical approach, assuming that the fatigue damage occurs at a site depending only on the stress distribution, can be obviously questioned. As a matter of fact, it has recently been shown that the crack initiation occurs in a subskin region for a fatigue test in which a superficial cracking is normally expected.[3]

In Part I of this paper, we localized and precisely identified the morphological strates of injection-molded PP samples differing by their molecular weight or injection conditions. Now, we shall study the fatigue behavior of these samples in order to establish its eventual relationships with the structure.

Journal of Applied Polymer Science, Vol. 34, 19–36 (1987)

CCC 0021-8995/87/010019-18$04.00

EXPERIMENTAL

The materials, test specimens, injection molding conditions, and resulting morphologies have been described in Part I of this paper. The most important data will be recalled in the Discussion section. The same analytical methods, DSC and WAXS on microtome sections, will be used to characterize the morphological changes due to fatigue. We added the three following methods of investigation:

—Scanning electronic microscopy (SEM). Fatigue tested specimens, which present cracks, were definitively broken in a tensile test. Then, the fracture surfaces were gold metallized and observed by SEM (JEOL 200 T). The first number at the bottom right of the photographs is the length of the white straight line (μm).

—Residual stress measurements. We used the method consisting of machining thin superficial layers and measuring the sample deformation resulting of the new stress distribution. This method has been widely used in polymers[4,5] including PP.[6] In our case, high precision measurements were made with a rugosimeter (Perthometer S6P, inductive system with a ball of 3 mm diameter and a pressure force of 6 mN).

—Fatigue testing. We used a laboratory made universal fatigue machine especially designed for polymer and composite testing.[7] We shall report only the results of flexural test at constant strain amplitude. The frequency was 28 Hz, the temperature 20 ± 2°C, and the relative humidity 50%. In these conditions, no self-heating is observable. Four samples were studied simultaneously. The induced stresses were continuously recorded, and the zone of maximum stress observed by stroboscopy, which allows to detect the onset of

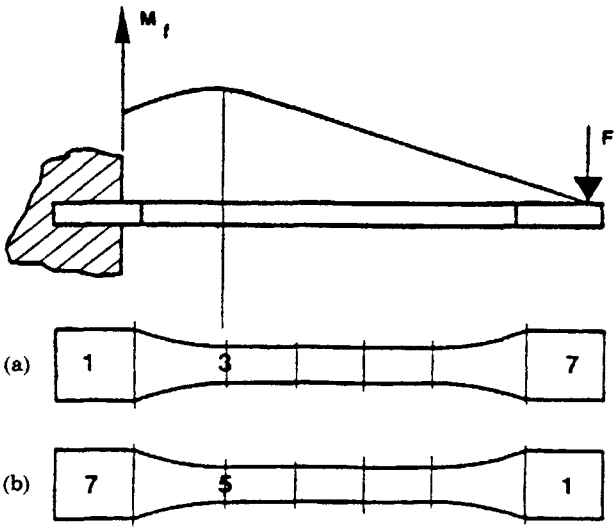

Fig. 1. Distribution of flexural moments along the tensile bar. Testing of zones 5 [Fig. 1(a)] and 3 [Fig. 1(b)].

cracking and, if necessary, to stop the machine in order to make SEM and analytical measurements.

The layer of crack initiation (CIL) was localized by optical microscopy; its depth is reproducible for the four samples under study.

The nonsymmetric longitudinal distribution of flexural moments along the calibrated section of the tensile specimens (Fig. 1) allows us to differentiate zones 3 (near the injection gate) and 5 (near the opposite head), which are not morphologically equivalent in the case of single gated molding.[8]

RESULTS

Residual Stresses

The residual stress intensity is in all cases smaller than 1 MPa as found by Coxon and White.[6]

VISUAL OBSERVATION OF THE CRACKING ZONE

The number of cracks and the time at which they appear differ noticeably from one sample to another. The results of these observations are summarized in Table I.

TABLE I
Morphological and Fatigue Characteristics[a] of Samples under Study and Correlation between Depths of CIL and A_{max}[b]

Sample	PP 5/82	PP 12/82	PP 12/82	PP 12/83	PP 12/83	PP 40/83
Most strained section	5	5	3	5	3	5
$M_n \times 10^{-3}$	72	53	53	53	53	53
$M_w \times 10^{-3}$	231	220	220	220	220	158
Depth of A_{max} (μm)	240	240	300	250	60	220
Depth of x_c max (μm)	140	100	—	230	—	230
Depth of x_c min (μm)	300	260	—	500	—	500
Depth of the crack initiation locus (μm)	220	250	280	270	110	210
Time to fracture (h)	500	160	80	600	200	140
Time at which cracking appears (h)		50	40	400	90	50
Number of cracks	1	Numerous	Numerous	1–2	Few	Numerous

[a] For a strain amplitude of 12×10^{-3}
[b] See test.

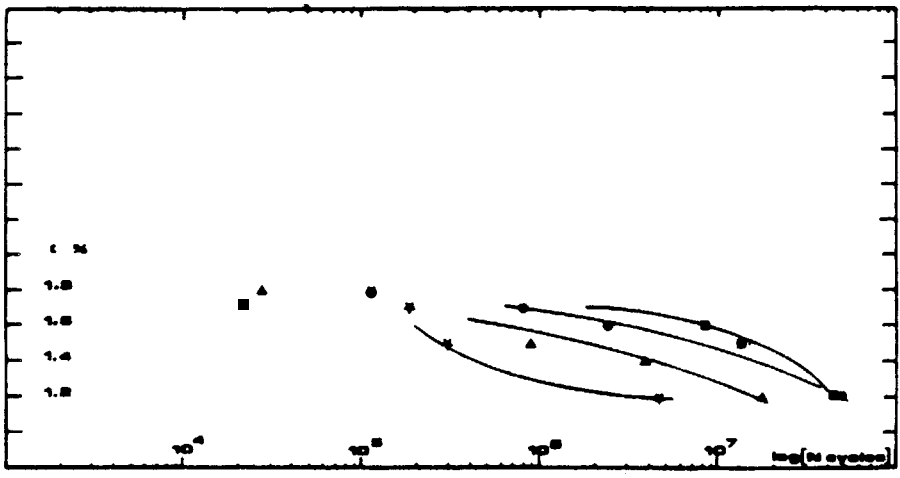

Fig. 2. Endurance curves for section 5 of the samples (1G5) under study: (■) 2a: PP 5/82; (▲) 2b: PP 12/82; (●) 2c: PP 12/83; (★) 2d: PP 40/83.

FATIGUE LIFETIME

Some endurance curves are shown in Figure 2 for zone 5 and in Figure 3 for zone 3. They call for the following comments:

- Influence of molecular weight. The stress-number of cycles to failure (N) curves display a pseudo-asymptote whose ordinate (stress endurance limit) is almost independent of the molecular weight: $\sigma_\infty \simeq 20$ MPa. In contrast, for a given strain amplitude, the fatigue lifetime increases with the molecular weight as shown in Table I for a strain amplitude $\epsilon = 12 \times 10^{-3}$($\epsilon = \Delta l/l$ = maximum strain of the outer layer of specimen).
- Influence of the longitudinal morphological heterogeneity: The fatigue lifetimes of the two zones under study are given in Table I. It can be observed

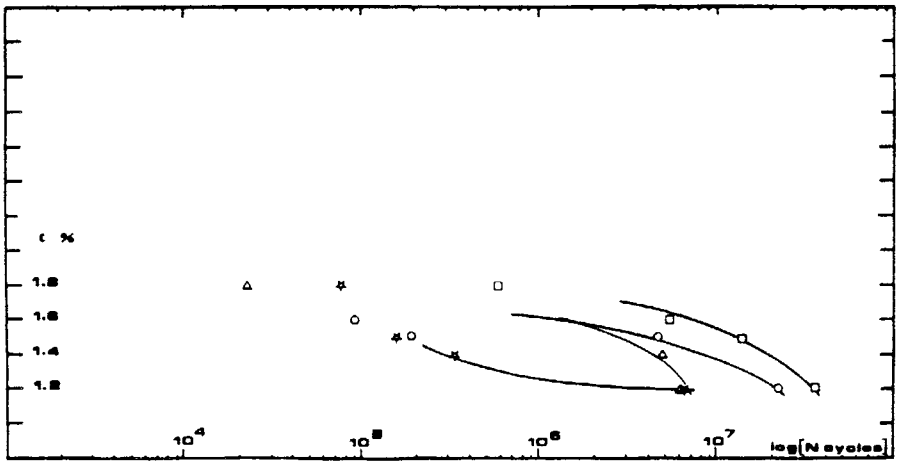

Fig. 3. Endurance curves for section 3 of the samples (1G3) under study (□) 3a: PP 5/82; (△) 3b: PP 12/82; (○) 3c: PP 12/83; (★) 3d: PP 40/83.

that zone 3 (close to the injection gate) is generally less resistant than the zone 5.

- Influence of injection conditions: The fatigue lifetime is almost four times longer for PP 12/83 than for PP 12/82 (Table I). It must be remembered that the conditions "82" and "83" differ essentially by the injection rate and holding pressure.

SEM OBSERVATIONS

Micrographs taken at the onset of cracking are presented in Figure 4. It appears clearly that the cracks initiated in the subskin region (a) and do not emerge at the surface as shown, by Watkinson et al.,[3] using optical microscopy. Despite the semicrystalline character of the polymer, a crazing zone (b) can be distinguished at the front of cracking. In Figure 5 craze fibrillation (a), as in the case of tensile tests[9] and a plastic zone (b) can be observed at the front of the crack.

In Figure 6 we can see: (a) a micrograph of a sample taken just before its fatigue fracture showing an emerging craze, crossing the amorphous skin and containing fibrils; (b) a slaky structure of crazes and fibrils between.

MORPHOLOGICAL CHANGES DURING FATIGUE

The results of analytical measurements on microtome cuts of the stressed sections can be summarized as follows:

- The depth distribution of the crystalline orientation index (A) determined by WAXS is shown in Figure 7. A very sharp decrease due to fatigue is observed in the crack initiation layer (CIL).
- This result is confirmed by IR dichroïsm measurements (Figure 8). Both crystalline and amorphous orientations decrease during fatigue. Indeed, for the initially less oriented PP/40, small change is observable.
- The changes of orientation factor (from IR measurements) along the calibrated part in the case where the section 5 is the most strained are shown in Figure 9. It appears clearly that the local orientation decay is correlated with the local strain (see Fig. 1).
- The changes of overall degree of crystallinity (from DSC measurements) are shown in Figure 10. A small but significant increase of x_c is observed; however, the shape of its depth distribution is not affected.

DISCUSSION

Loci of Crack Initiation

It could initially be hypothesized that the fatigue behavior was linked with the residual stress distribution in the samples. The results of residual stress measurements showed however that this factor can be practically neglected. Table I summarizes some data on the initial morphology and fatigue results (for a strain amplitude of 12×10^{-3}). It can be clearly observed that the depth of the CIL is well correlated with the depth of the maximum of crystalline orientation index (A_{max}) (Table I). Then, the following interpretation can be proposed. In a flexural mode of fatigue, the skin undergoes the

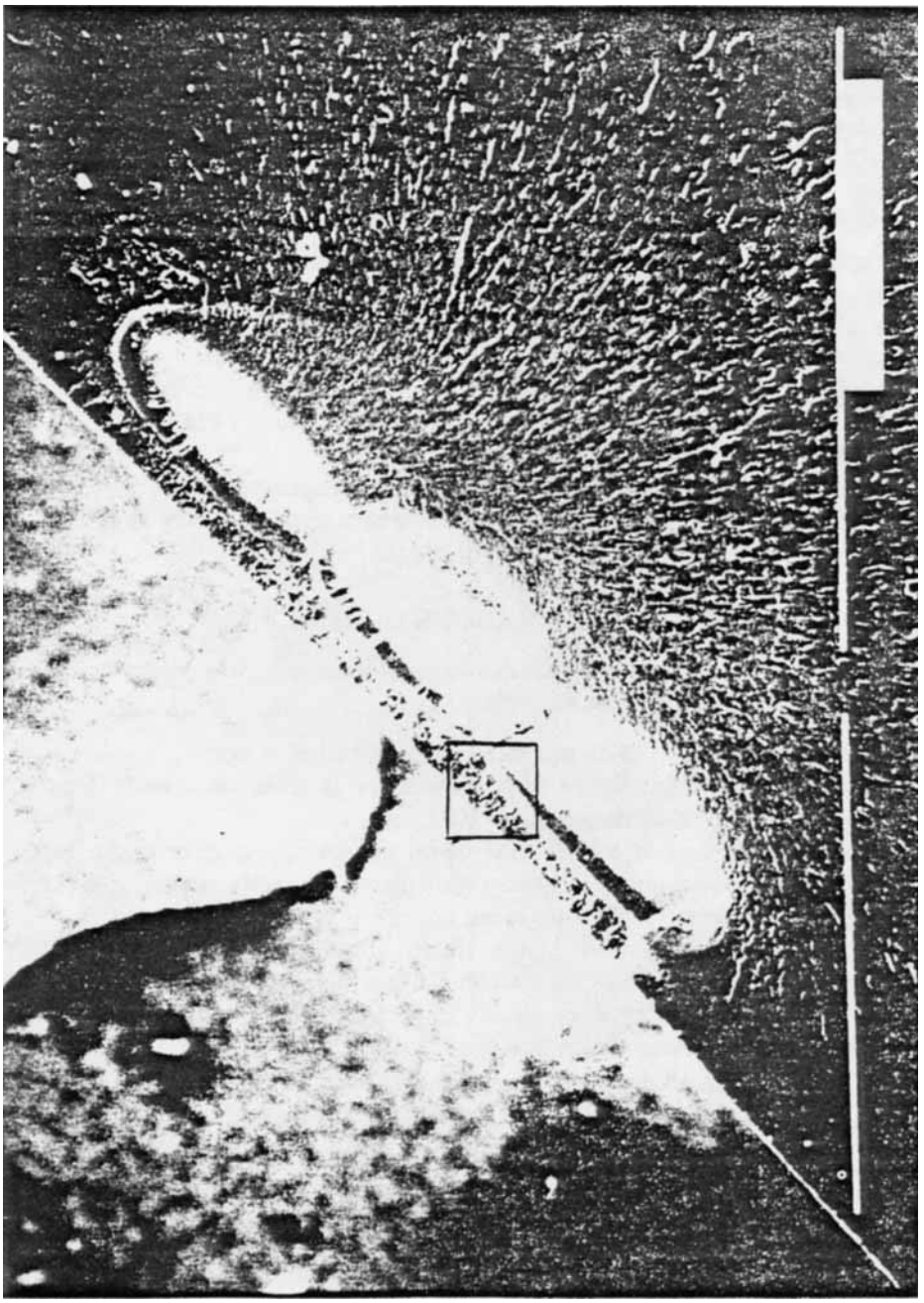

(a)

Fig. 4. Micrographs of fracture surfaces for fatigue tested specimens just after crack apparition: (4a) crack initiation in subskin region; (4b) crazing zone.

(b)

Fig. 4. *(Continued from the previous page.)*

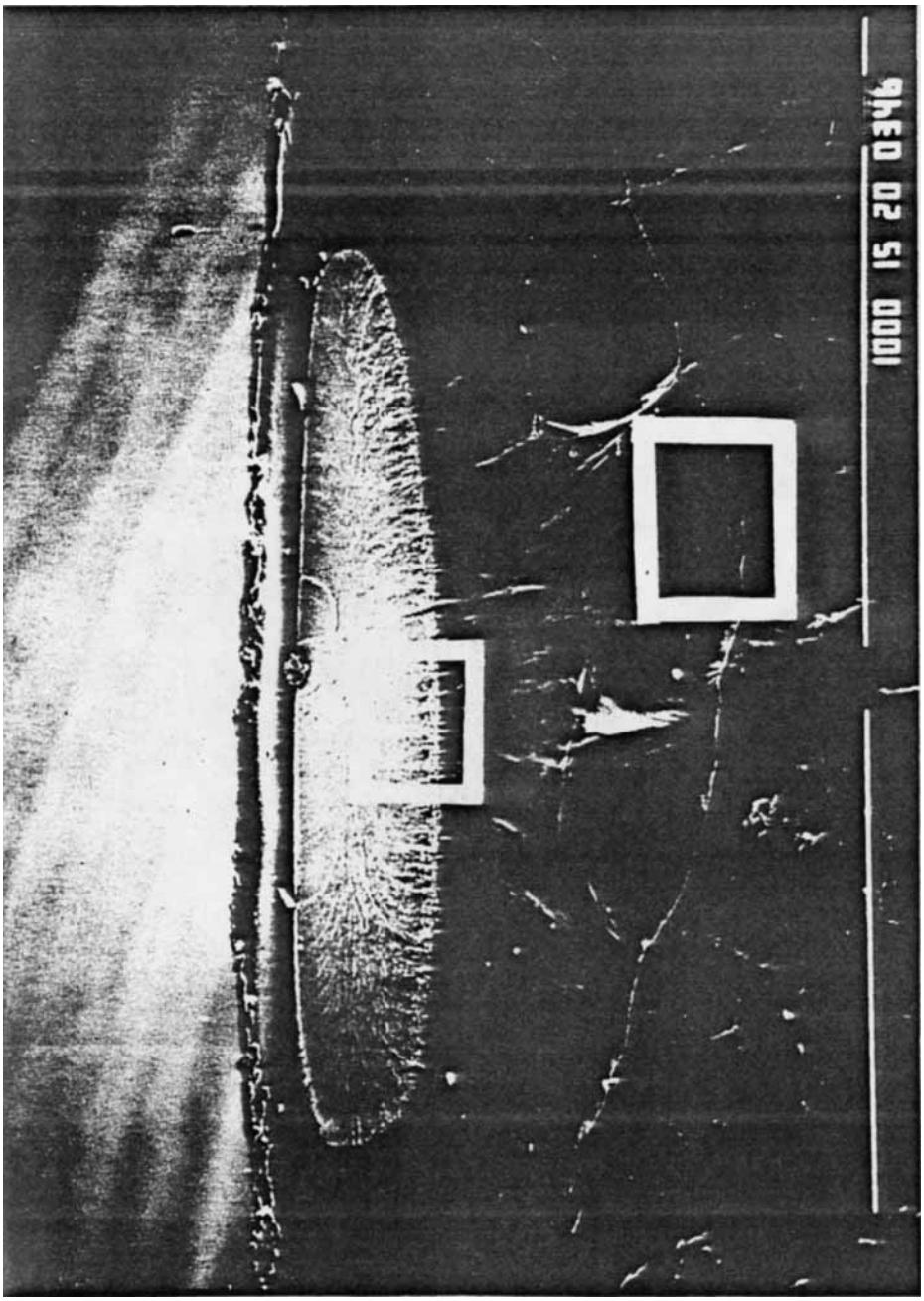

Fig. 5. Micrographs of fracture surfaces for fatigue tested specimens just after crack apparition: (5a) fibrillation zone; (5b) plastic zone.

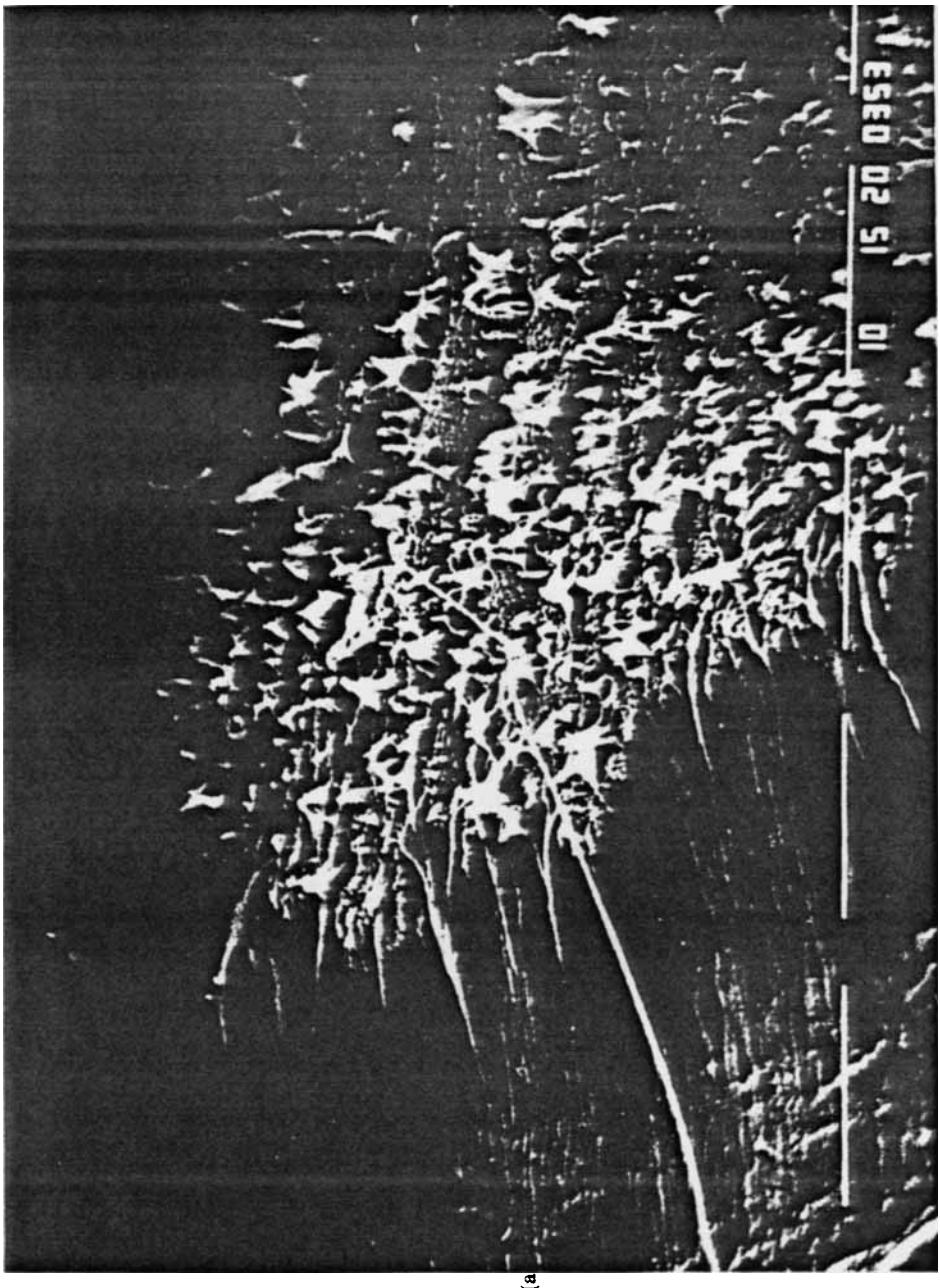

(a

Fig. 5. *(Continued from the previous page.)*

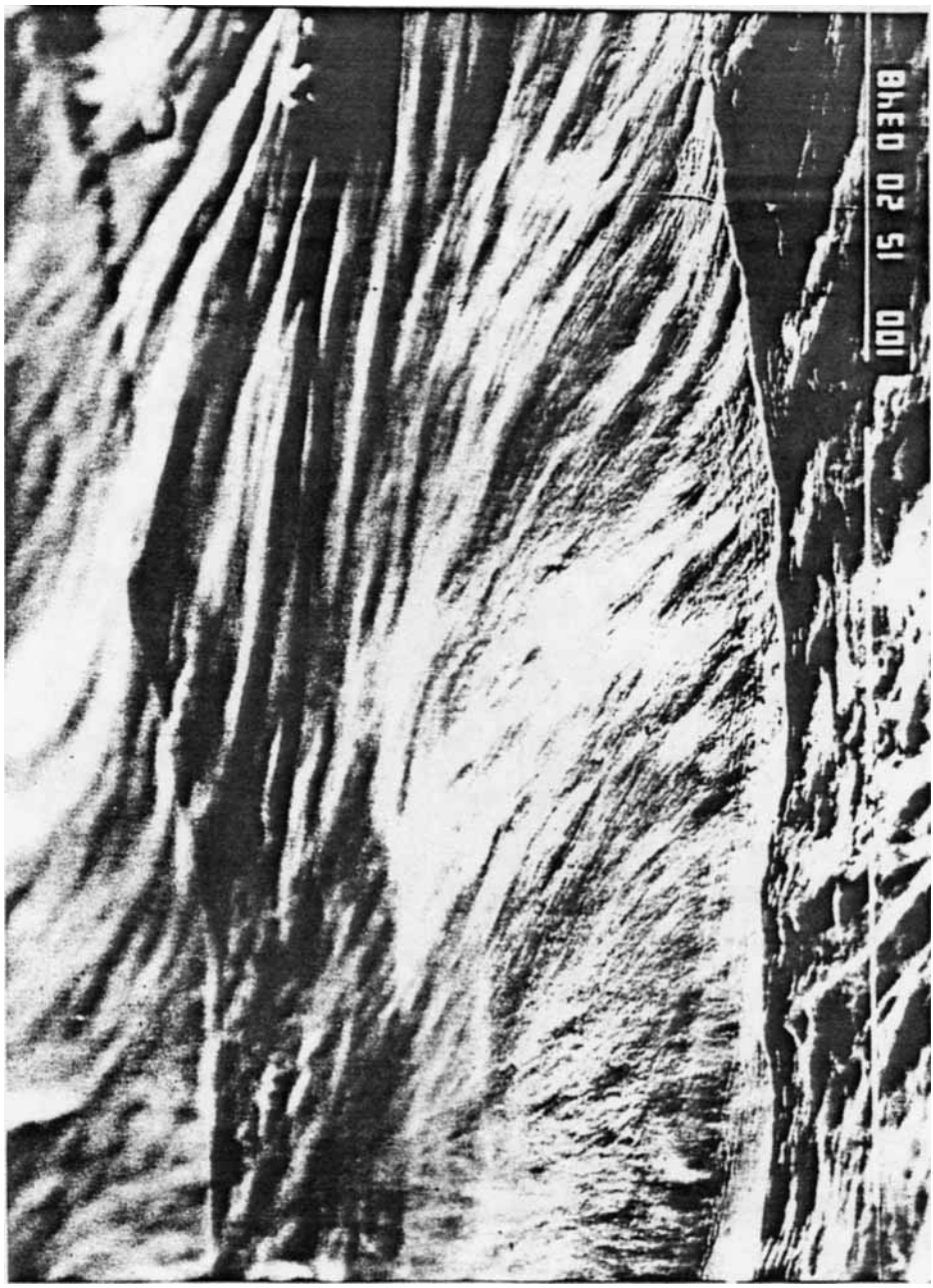

(b)

Fig. 5. (*Continued from the previous page.*)

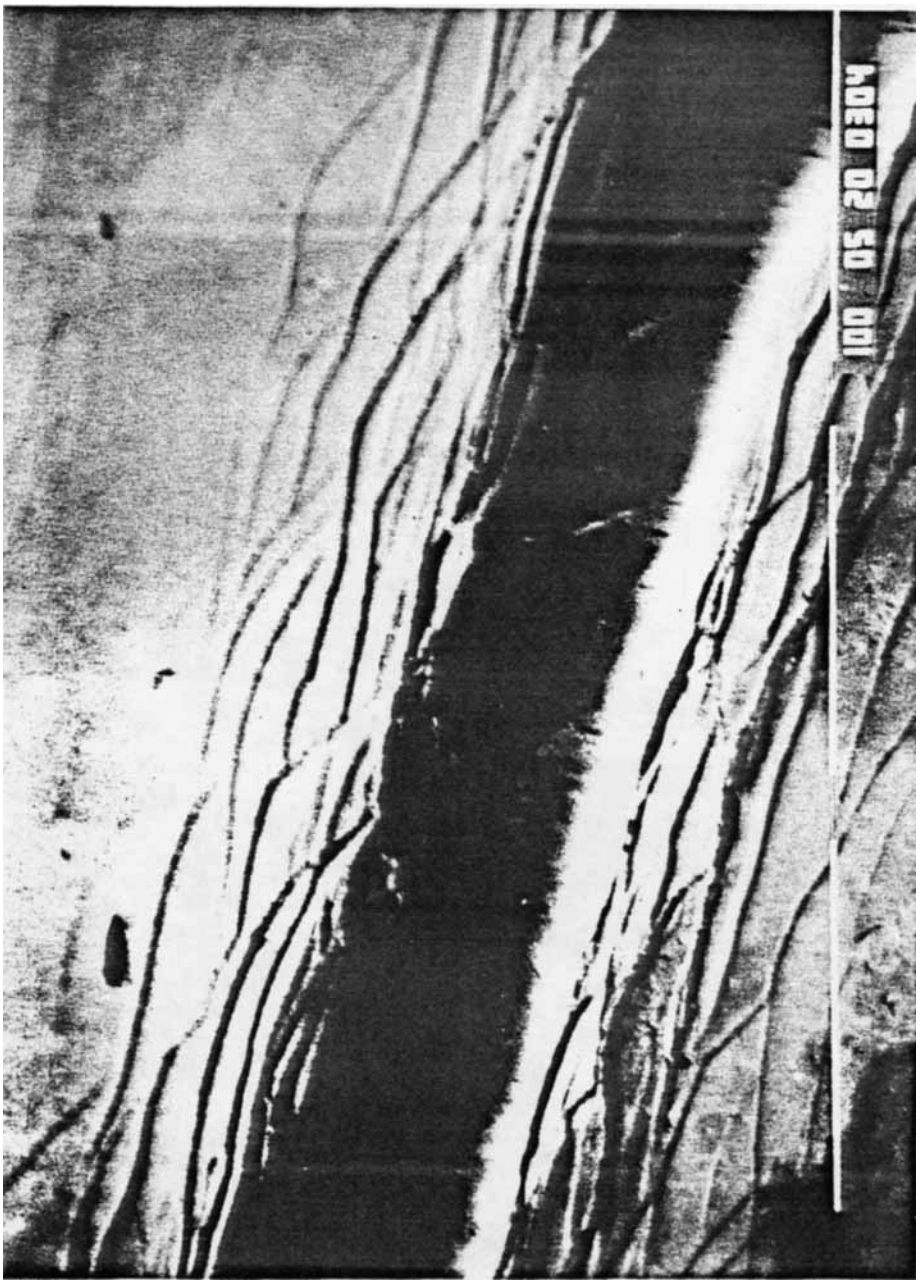

Fig. 6. Micrographs of fracture surfaces of fatigue tested specimens just before failure: (6a) emerging craze; (6b) slaky structure of crazes.

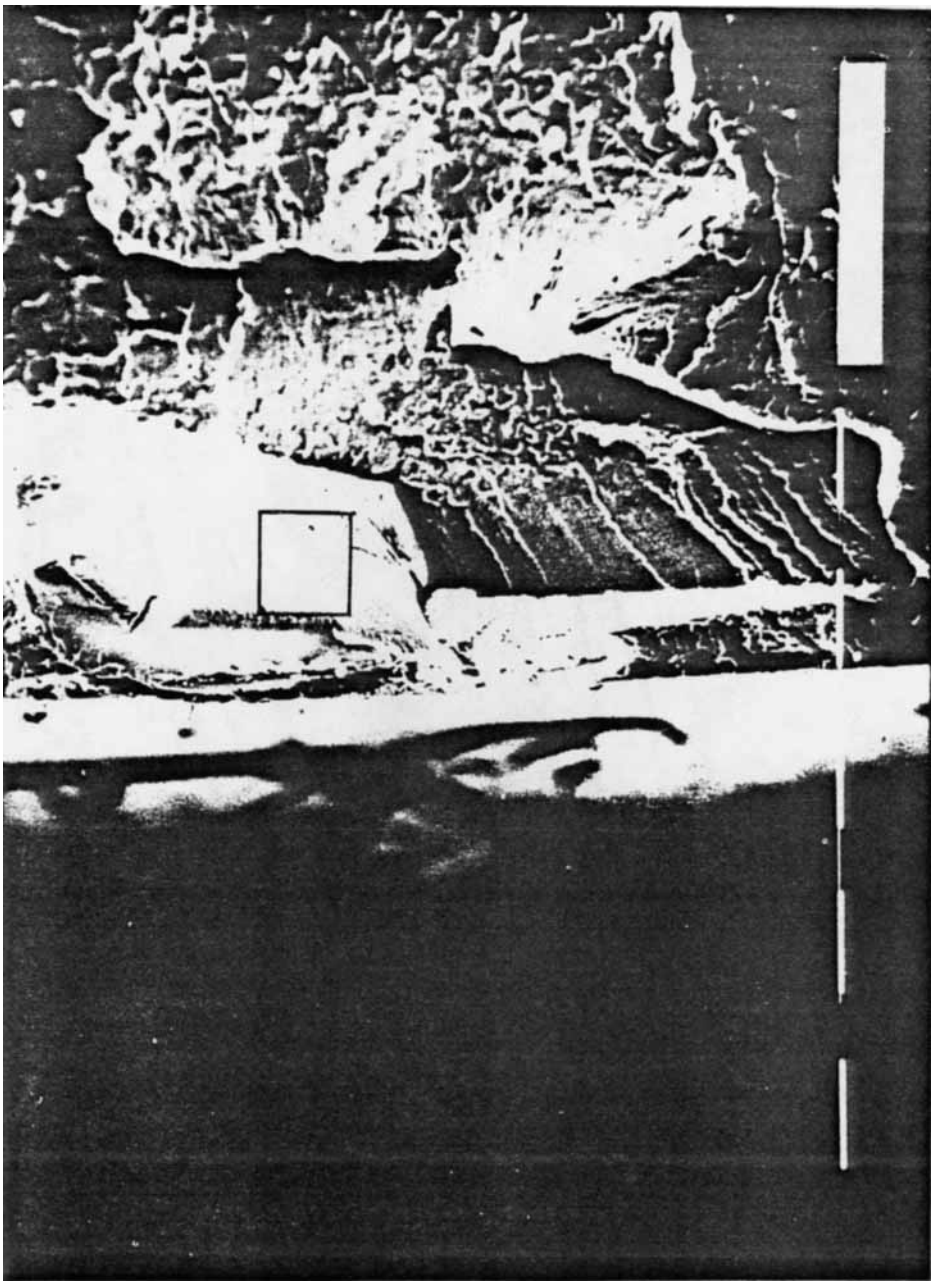

(a)

Fig. 6. *(Continued from the previous page.)*

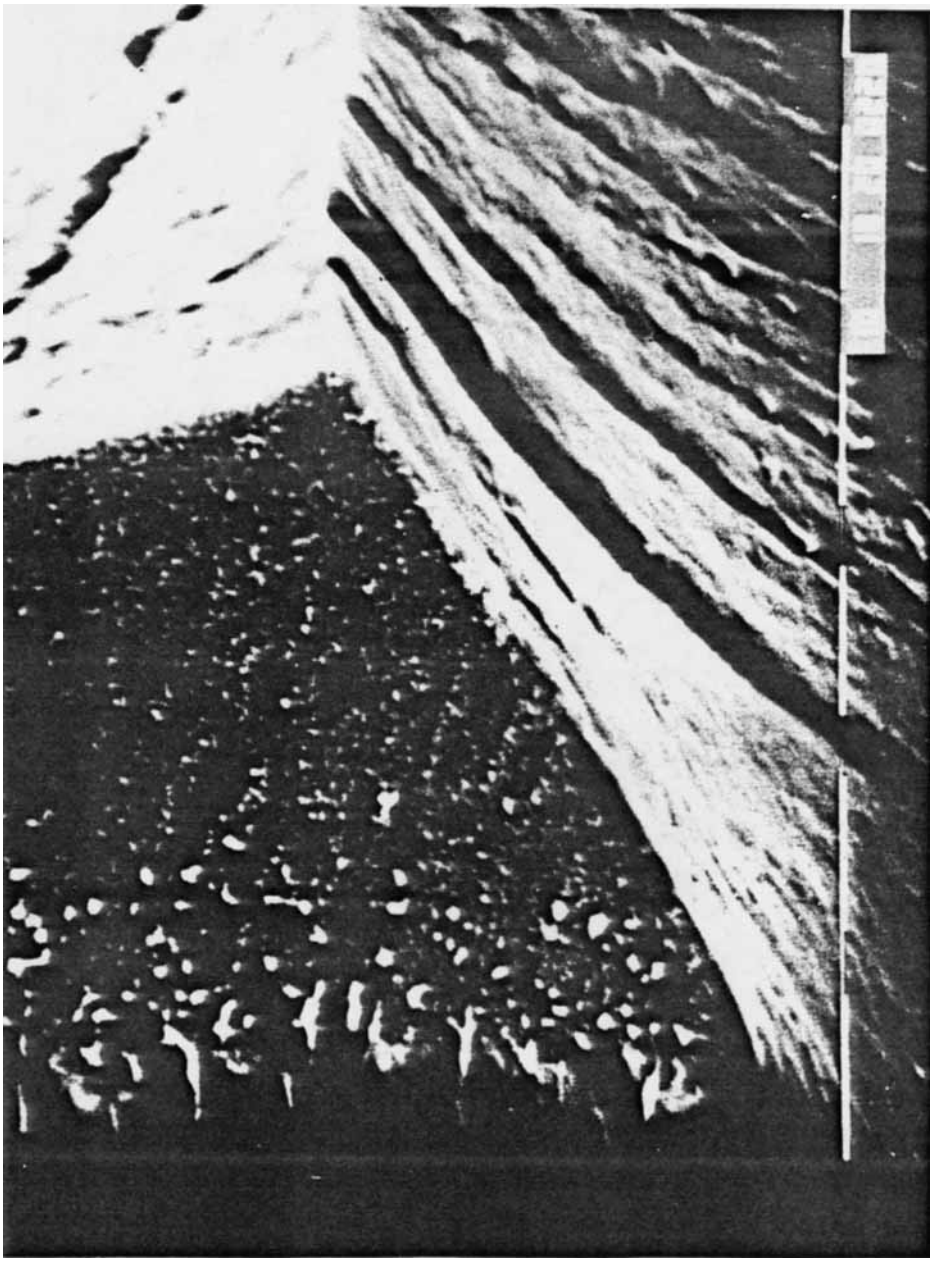

(b)

Fig. 6. *(Continued from the previous page.)*

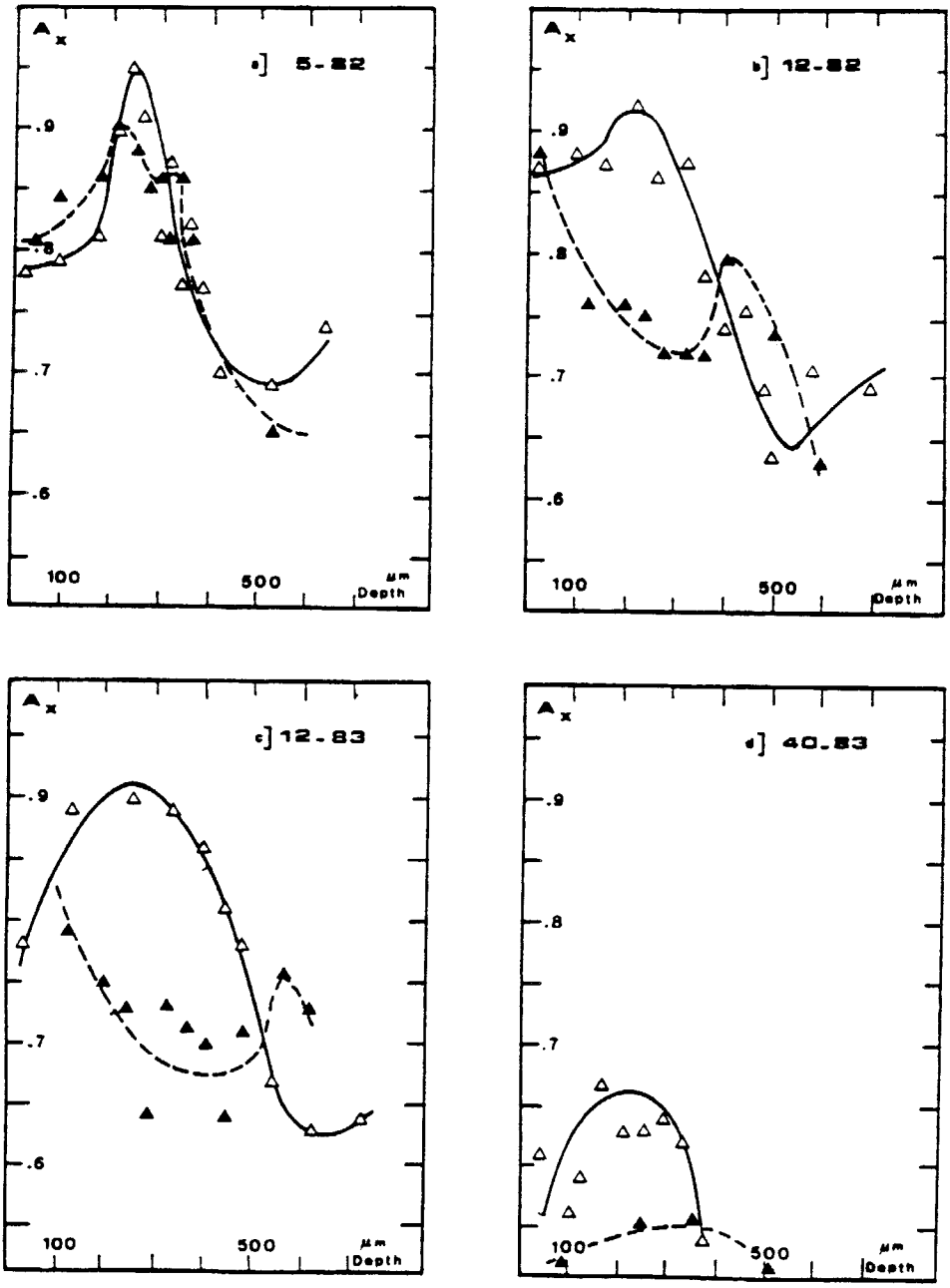

Fig. 7. Depth distribution of the crystalline orientation index A, before (△) and after (▲) fatigue testing: (7a) PP 5/82; (7b) PP 12/82; (7c) PP 12/83; (7d) PP 40/83.

maximum strain. However, above its glass transition temperature ($T_g \simeq 0°C$), this layer of high amorphous content is ductile and can be submitted to high deformations without any damage. The layer of A_{max} undergoes smaller strains, but, owing to its high mechanical anisotropy, its ultimate elongation is minimum in the stress direction, which coïncides, in our test, with the direction of crystalline orientation. Thus, it is not surprising to find systematically the crack initiation loci in this zone.

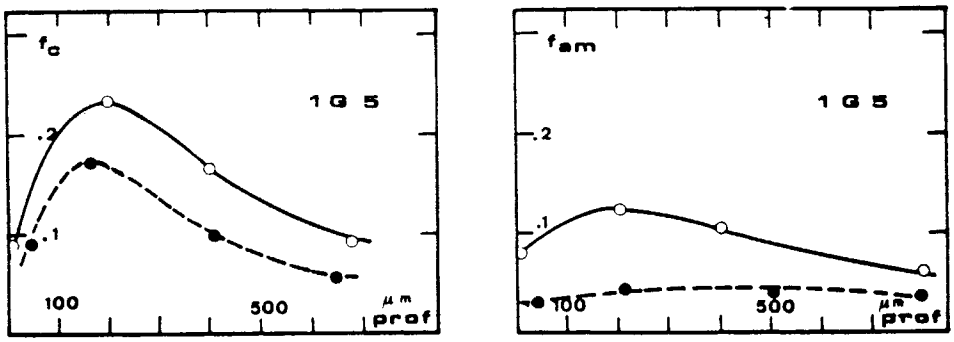

Fig. 8. Depth distribution of crystalline and amorphous orientations factors from IR dichroïsm measurements before (○) after (●) fatigue testing (PP 12/82).

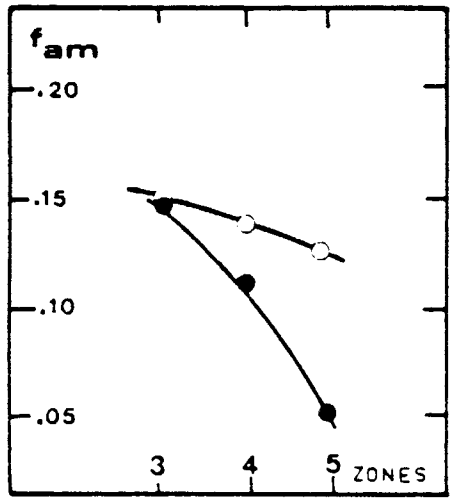

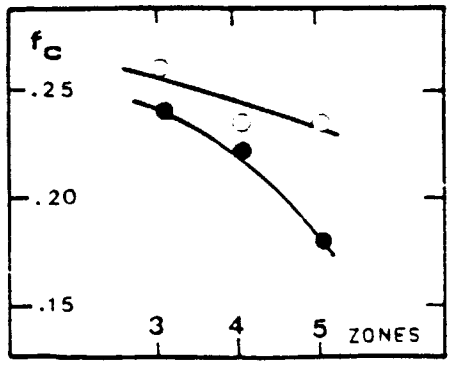

Fig. 9. Orientation decay due to fatigue along the longitudinal axis of the samples (○) before and (●) after fatigue testing (PP 12/82).

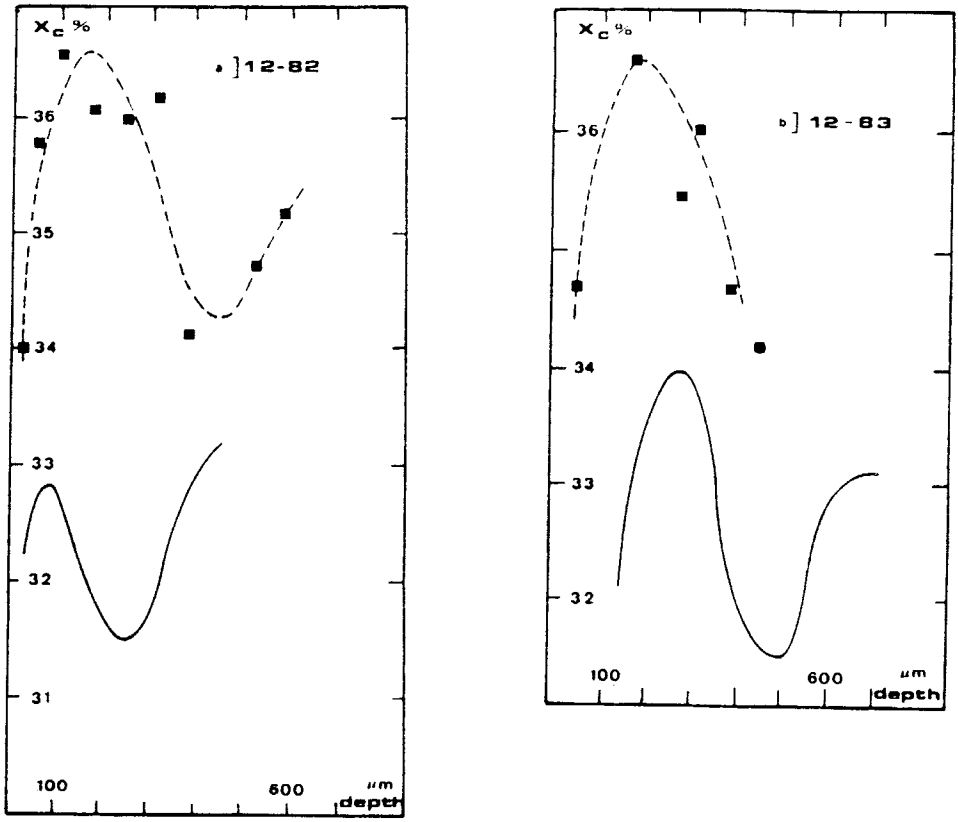

Fig. 10. Depth distribution of the degree of crystallinity, X_c, before and after (■) fatigue testing: (10a) PP 12/82; (10b) PP 12/83.

Since the deeper the layer of A_{max}, the smaller the local strain, a considerable influence of the skin-core structure on the fatigue behavior is to be expected. This is well illustrated by the difference existing between the durabilities of sections 3 and 5 of PP 12/83, depth of A_{max} = 250 µm in section 5 against 60 µm in section 3, time to fracture, 600 h section 5 against 200 hours section 3 (Table I). Similar observations have been made in the case of PVDF.[10]

MICROSTRUCTURAL CHANGES IN THE CRACK INITIATION ZONE

Our main experimental results concern the loss of orientation in the CIL. They can be discussed on the basis of the Peterlin model[11] and observations of Samuels[12] on the influence of amorphous orientation in the fracture of uniaxially oriented PP films.

The data on initial morphology suggest that, in the CIL, the crystallites are packed in the stress direction and connected by tie molecules of almost identical orientation, eg, of low ultimate elongation. These tie molecules are therefore easily broken, which allows the crystallites to take any equilibrium position depending for instance on the local nonuniform stress distribution.

These results of DSC and WAXS measurements show that no shear destruction of crystallites occurs. The only phase transfer consists in a slight post-crystallization (Fig. 9), presumable a lamellae thickening favored by the local stress-induced free volume creation and, perhaps, some chemicrystallization accompanying the rupture of tie molecules.

MECHANISM OF CRACK FORMATION

As shown in Table I, two families of fatigue behavior can be clearly distinguished. The first one (H) PP 5/82 and PP 12/83 is characterized by the formation of a small number of cracks and long "induction" time before the appearance of a crack. The second one (L) PP 12/82 and PP 40/83 is characterized by the formation of numerous cracks and a short "induction" time. This suggests that two very different kinetic regimes of cracking exist. According to Schultz,[13] they could correspond to two types of initiation sites: one (H) of low concentration responsible for the cracking of the first family, the other (L) of higher concentration, but which can be activated only in the second family. Its seems reasonable to suppose, from our results, that the activation of "L" sites is easier when the molecular weight is low. This is consistent with a mechanism involving a scission of tie molecules since the higher the molecular weight, the higher the tie molecules concentration.

In our test conditions, the PP 12 would be located at the transition between the two mechanisms H and L, its fatigue behavior depending on the subskin morphology which finally depends on processing conditions. As a matter of fact, Sandt[14] finds that the spherulite boundary and intercrystallite cracking are almost equiprobable for the strain rate under study ($\simeq 5 \times 10^{-2}$ m/s) for PP samples.

If we consider that the most important parameter is the molecular weight of the polymer, the Schultz scheme[13] allows us to attribute the first mechanism (spherulite boundary cracking), to the family L, and the second one (intercrystallite cracking), to the family H. Unfortunately, no clear confirmation can be obtained from our SEM observations, owing to the very specific morphology (fine, more or less distinguishable row nucleated spherulites) of the CIL.

CONCLUSION

The peculiar aspects of the fatigue behavior of PP injection-molded samples, essentially the subskin crack initiation, are well explained by the "fine" skin-core structure as established in the first part of this paper. It appears that, at least for the samples of intermediary molecular weight (PP/12), a change in processing conditions can lead to a change in cracking mechanisms and, consequently, a considerable change in durability. Similar observations lead us to take into consideration the position of the stressed section of the part relatively to the injection gate.

References

1. R. J. Crawford and P. P. Benham, *J. Mater. Sci.*, **9**, 98 (1974).
2. Y. M. May, *J. Appl. Polym. Sci.*, **26**, 3947 (1981).
3. K. Watkinson, A. Thomas, and M. Bevis, *J. Mater. Sci.*, **17**, 347 (1982).

4. P. So and L. J. Broutman, *Polym. Eng. Sci.*, **16** (12), 785 (1976).
5. J. F. Mandell, K. L. Smith, and D. D. Huang, *Polym. Eng. Sci.*, **21** (17), 1173 (1981).
6. L. D. Coxon and J. R. White, *Polym. Eng. Sci.*, **20** (3), 230 (1980).
7. R. Gauvin and J. P. Trotignon, *J. Testing Evaluation ASTM*, **6**, 48 (1978).
8. J. P. Trotignon, J. L. Lebrun, and J. Verdu, *Plast. Rubber Process. Appl.*, **2** (3), 247 (1982).
9. B. Z. Jang, D. R. Uhlmann, and J. B. Vander Sande, *Polym. Eng. Sci.*, **25** (2), 98 (1985).
10. J. P. Trotignon and J. Verdu, in *17th Europhysics Conference on Macromolecular Physics*, Prague, July 1985.
11. A. Peterlin, *J. Polym. Sci. Part. C*, **32**, 297 (1970).
12. R. J. Samuels, *Polym. Eng. Sci.*, **19** (2), 66 (1979).
13. J. M. Schultz, *Polym. Eng. Sci.*, **24** (10), 770 (1984).
14. A. Sandt, *Kunststoffe*, **72**, 791 (1982).

Received March 14, 1986
Accepted July 10, 1986